



3 1176 00106 4592


NACA

RESEARCH MEMORANDUM

TRANSONIC WIND-TUNNEL INVESTIGATION OF THE AERODYNAMIC
LOADING CHARACTERISTICS OF A 60° DELTA WING IN THE
PRESENCE OF A BODY WITH AND WITHOUT INDENTATION

By John P. Mugler, Jr.

Langley Aeronautical Laboratory
Langley Field, Va.

*NACA Res also
7 R/N-121*

*effective
Oct. 14, 1957*

RM 11-15-57

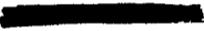
CLASSIFIED DOCUMENT

This material contains information affecting the National Defense of the United States within the meaning of the espionage laws, Title 18, U.S.C., Secs. 793 and 794, the transmission or revelation of which in any manner to an unauthorized person is prohibited by law.

NATIONAL ADVISORY COMMITTEE FOR AERONAUTICS

WASHINGTON

September 15, 1955


NATIONAL ADVISORY COMMITTEE FOR AERONAUTICS

RESEARCH MEMORANDUM

TRANSONIC WIND-TUNNEL INVESTIGATION OF THE AERODYNAMIC
LOADING CHARACTERISTICS OF A 60° DELTA WING IN THE
PRESENCE OF A BODY WITH AND WITHOUT INDENTATION

By John P. Mugler, Jr.


SUMMARY

An investigation was conducted in the Langley 8-foot transonic pressure tunnel to determine the aerodynamic loading characteristics of a 60° delta wing in the presence of a body with and without body indentation in accordance with the transonic-area-rule concept. The wing loads were measured with a strain-gage wing balance. The tests covered a Mach number range from 0.6 to 1.2 and an angle-of-attack range from 0° to 20° at a Reynolds number of about 3.6×10^6 based on the wing mean aerodynamic chord. The wing had 60° sweepback of the leading edge, an aspect ratio of 2.31, a taper ratio of 0, and NACA 65A003 airfoil sections parallel to the model plane of symmetry.

Significant center-of-pressure movements were observed at pitch-up and in the transonic Mach number range. At pitch-up, the center of pressure experienced abrupt forward and inboard movements of the order of 4 percent of the wing mean aerodynamic chord and 3 percent of the wing semispan, respectively. Increasing the Mach number through the transonic speed range was accountable for rearward and outboard center-of-pressure movements of the order of 7 percent of the mean aerodynamic chord and 3 percent of the semispan, respectively. Body indentation had no significant effects on the aerodynamic loading characteristics. The effects of Mach number and body indentation on the division of load between the wing and body were small.

INTRODUCTION

Designers of transonic and supersonic airplanes require knowledge of the effects of plan-form variables on the aerodynamic loading characteristics of wings at transonic speeds. Present theoretical methods



for predicting the aerodynamic loadings for wings in this speed range are not proven. Therefore, a systematic research investigation is being conducted in the Langley 8-foot transonic pressure tunnel to determine the effects of wing geometric parameters on the aerodynamic loading characteristics of wings at transonic speeds. References 1 and 2 present results that show the effects of taper ratio and body indentation, and sweep and thickness ratio, respectively, on the loading characteristics. This paper presents the results of the third phase of this general investigation and shows the aerodynamic loading characteristics of a 60° delta wing. Since remarkable aerodynamic gains are being obtained through the application of the transonic area rule (ref. 3), a study of the effect of body indentation on the wing loads was included. This was accomplished by testing the delta wing in the presence of an unindented and an indented body.

The wing loads were determined by utilizing a strain-gage wing balance which measured normal force, pitching moment, and bending moment of the wings. From these results the location of the center of pressure was determined. In addition, the division of normal-force and pitching-moment loads between the wing and the body was determined, since overall force-test data from tests of the same configuration were available.

SYMBOLS

M	free-stream Mach number
N_W	normal force on wing in presence of body, lb
N_B	normal force on body in presence of wing, lb
N_{WB}	normal force on wing-body combination, lb
M_W	pitching moment of wing in presence of body about $0.25\bar{c}$, in-lb
M_{WB}	pitching moment of wing-body combination about $0.25\bar{c}$, in-lb
M_{BM}	bending moment for a wing panel in presence of body about body center line, in-lb
C_{N_W}	normal-force coefficient for wing in presence of body, N_W/qS
C_{N_B}	normal-force coefficient for body in presence of wing, N_B/qS

- $C_{N_{WB}}$ normal-force coefficient for wing-body combination, N_{WB}/qS
- C_{m_W} pitching-moment coefficient for wing in presence of body,
 $M_W/qS\bar{c}$
- $C_{m_{WB}}$ pitching-moment coefficient for wing-body combination, $M_{WB}/qS\bar{c}$
- C_{BM} bending-moment coefficient for a wing panel in presence of
 body, $\frac{M_{BM}}{q \frac{S}{2} \frac{b}{2}}$
- $\frac{y}{b/2}$ lateral position of center of pressure in fraction of wing
 semispan measured from body center line, C_{BM}/C_{N_W}
- x/\bar{c} longitudinal position of center of pressure in fraction of
 mean aerodynamic chord measured from leading edge of mean
 aerodynamic chord, $0.25 - \frac{C_{m_W}}{C_{N_W}}$
- \bar{c} wing mean aerodynamic chord (with rounded tips),
 $\frac{2}{144S} \int_0^{b/2} c^2 dy$, in.
- c_{av} wing average chord (with rounded tips),
 $\frac{\text{Root chord} + \text{Tip chord}}{2}$, in.
- c local chord, in.
- D_{max} maximum body diameter, in.
- $b/2$ semispan of total wing (with rounded tips), in.
- S area of total wing (with rounded tips and including area
 blanketed by body), sq ft
- x longitudinal distance parallel to model center line, in.
- y lateral distance measured perpendicular to model center line, in.
- q free-stream dynamic pressure lb/sq ft

- R Reynolds number based on wing mean aerodynamic chord
- α angle of attack of wing-body center line, deg

APPARATUS AND METHODS

Tunnel

The test section of the Langley 8-foot transonic pressure tunnel is rectangular in cross section and has a cross-sectional area of approximately 50 square feet. The upper and lower walls of the test section are slotted to permit continuous operation through the transonic speed range. Some details of the test section are shown in figure 1. During this investigation, the tunnel was operated at approximately atmospheric stagnation pressure. The dewpoint of the tunnel air was controlled and was kept at approximately 0° F. The stagnation temperature of the tunnel air was automatically controlled and was kept constant and uniform across the tunnel at 120° F. Control of both dewpoint and stagnation temperature in this manner minimized humidity effects. The axial distribution of Mach number in the vicinity of the model was satisfactorily uniform at all test Mach numbers. Local deviations from the average stream Mach number were no larger than 0.005 at subsonic speeds. With increases in Mach number above 1.0, these deviations increased but did not exceed 0.010 in the region of the wing at the highest test Mach number of 1.2. Tests reported in reference 4 indicate that local flow nonuniformities of this magnitude have no effect on the measured force data. Some representative Mach number distributions at the center of the test section are presented in figure 2.

Models

The delta wing tested has 60° sweepback of the leading edge, a taper ratio of 0, and NACA 65A003 airfoil sections parallel to the model plane of symmetry. The actual wing deviated from the theoretical delta plan form in that the wing tips were rounded. Rounding the tips reduced the wing area by a small amount (a reduction of 0.005 sq ft) and produced negligible changes in mean aerodynamic chord length and location. The original semispan of 9.118 inches, however, was reduced to 8.587 inches; a reduction of approximately 6 percent. In this paper the bending-moment coefficients and the lateral center-of-pressure locations are based on the actual semispan of 8.587 inches. The theoretical aspect ratio, which assumes pointed wing tips, is 2.31. Dimensional details of the wing-body combinations are presented in figure 3. The wing was constructed of steel and was tested as a midwing configuration.

The delta wing was tested in the presence of two bodies designated basic and indented. The body frame was constructed of steel and housed an internal strain-gage wing balance. Both left and right wing panels were mounted on this balance independent of the body. The balance measured bending moment on each wing panel and normal force and pitching moment on both wing panels. Figure 4 shows a photograph of the wing balance mounted in the body. The outer shell of the body was constructed of a plastic type material between body stations 22.5 and 36.9 inches. Change in body configuration was made by replacing the outer plastic shell with a different outer plastic shell. The shape of the indented body was derived by application of the transonic area rule (ref. 3) for a Mach number of 1.0. A photograph of the delta wing in the presence of the basic body is presented in figure 5. Body coordinates for both the basic and indented body are presented in table I.

When a plastic body shell was put into place, a gap of approximately 0.030 inch was left between the wing surface and the body shell all around the wing in order that there would be no physical interference (see section A-A, fig. 3). The base of both body configurations was sealed to prevent any flow of air through this gap and out of the base of the body. An electrical system to determine if the body fouled the wing under high loading conditions incorporated painting the wing cut-out in the body shell with a conductive silver paint. If fouling occurred, data were not recorded.

The model was attached to the tunnel central support system by means of a sting (fig. 1). This type of support system keeps the model near the center line of the tunnel throughout the angle-of-attack range.

Measurements and Accuracy

A study of the factors affecting the accuracy of the results indicates that the measured coefficients are accurate within the following limits:

M	C_{N_W}	C_{m_W}	C_{BM}
0.6	0.009	0.004	0.008
1.2	.004	.002	.004

The average stream Mach number was held to within ± 0.003 of the nominal values shown on the figures; generally, this deviation did not exceed ± 0.002 . As previously stated, during the tunnel description,

the local deviations from the average stream Mach number ranged from 0.005 at subsonic speed to 0.010 in the region of the wing at the highest test Mach number of 1.2.

The angle of attack of the model was measured with a strain-gage attitude transmitter mounted in the model nose. A consideration of factors affecting the accuracy of this measurement indicates that the model angle of attack is accurate to within $\pm 0.1^\circ$ relative to the free stream.

A quantitative effect of the gap at the wing-body juncture was not evaluated during these tests. Reference 1, however, shows such an evaluation with a similar width gap for two swept-wing configurations. A study of the data from reference 1 indicates that addition of seals to the configurations had some effects on the measured force and moment coefficients. The addition of seals decreased slightly the negative slope of the pitching-moment-coefficient curves and caused sizable differences above pitch-up; increased slightly the slope of the lift curve below pitch-up; and had negligible effects on the bending-moment coefficients below pitch-up.

The configurations tested were designed to be symmetrical. However, slight model asymmetries existed as shown by the pitching-moment and bending-moment curves of figures 7 and 8. Since center-of-pressure locations for the symmetrical cases were desired, the longitudinal and lateral centers of pressures were determined from moment curves that were shifted to pass through zero wing normal-force coefficient at zero-moment coefficient. This shift increased the accuracy of the computed center-of-pressure position in the low range of wing normal-force coefficients.

The configurations were tested through an angle-of-attack range from 0° to 20° and a Mach number range from 0.6 to 1.2 when not restricted by balance load limitations. The Reynolds number based on wing mean aerodynamic chord increased from 2.8×10^6 at a Mach number of 0.6 to 3.7×10^6 at a Mach number of 1.2 (fig. 6).

RESULTS

Force and moment coefficients for the 60° delta wing in the presence of the basic and indented body are presented in figures 7 and 8, respectively. From paired curves of force and moment coefficients the longitudinal and lateral center-of-pressure positions have been determined and presented in figures 9 and 10. The division of normal-force and pitching-moment loads between the wing and the body was determined by analysis of the data presented herein in conjunction with unpublished

data from an overall force test of an identical wing-body combination and is presented in figure 11. The unpublished data were also obtained in the Langley 8-foot transonic pressure tunnel and are of the same order of accuracy as the data presented herein.

In most instances too few data points were recorded in the region of pitch-up to rigidly define the force- and moment-coefficient curves. Therefore the force- and moment-coefficient curves in that region were faired with dashed lines utilizing data from reference 5 and unpublished data obtained on another delta-wing configuration in the Langley 8-foot transonic tunnel.

In order to facilitate presentation of the data, staggered scales have been used in many figures and care should be taken in selecting the zero axis for each curve.

DISCUSSION

With increases in C_{N_W} up to pitch-up, at a constant Mach number, the longitudinal center-of-pressure position remains essentially constant throughout the Mach number range, whereas, the lateral position experiences a slight inboard movement above a Mach number of 0.94 (fig. 9(a)). At pitch-up the center of pressure experiences rather abrupt forward and inboard movements of the order of 4 percent of the mean aerodynamic chord and 3 percent of the wing semispan, respectively. Above pitch-up further increases in C_{N_W} cause a gradual rearward and inboard center-of-pressure movement.

Generally, with increases in Mach number from 0.6 to approximately 0.85 at a constant C_{N_W} , the center of pressure experiences a gradual rearward movement (fig. 9(b)). Between Mach numbers of about 0.85 and 1.0 the onset of supersonic flow over the wing causes this rearward center-of-pressure movement to continue at a more rapid rate resulting in a transonic center-of-pressure shift of the order of 7 percent of the mean aerodynamic chord. The lateral position moves gradually outboard up to a Mach number of about 0.94 except at the higher wing normal-force coefficients. The transonic outboard movement of about 3 percent of the semispan is rather abrupt and occurs over a small range of Mach number (approx. 0.94 to 0.97). Above a Mach number of approximately 1.0 both the longitudinal and lateral center-of-pressure movement diminishes and the locations remain relatively constant in most instances.

The center-of-pressure loci for the two configurations are shown in figure 10, where the longitudinal position of the center of pressure is plotted against the lateral position. The accuracy of the data does

not justify the large plotting scale used in these figures. This scale was chosen only to separate the data sufficiently to make the effects of Mach number and wing normal-force coefficient distinct and evident in addition to presenting the longitudinal and lateral positions in the proper proportion to each other. The $c/4$ and c_{av} are shown in figure 10 for reference and orientation; \bar{c} is not shown on the main figure because its location is too far inboard. The center-of-pressure envelopes are shown in relation to the complete configurations in the sketch in the upper right position of the figures. The center-of-pressure bounds are in the same general location on the wing for both the basic and indented configurations.

Examination of figure 9 shows that body indentation had no significant effects on the loading characteristics. Several trends of a small order of magnitude, due to body indentation, can be noticed such as the slight delay in the Mach number for the transonic rearward center-of-pressure movement; the tendency of the longitudinal center-of-pressure location to move to a more rearward position (below pitch-up) at supersonic speeds; and the tendency for the lateral position to remain slightly inboard (below pitch-up) below a Mach number of about 1.10.

The division of normal-force and pitching-moment loads for both the basic and indented configurations (fig. 11) is presented as wing normal-force coefficient and pitching-moment coefficient for the wing and wing-body against the total normal-force coefficient for the wing-body combination. Examination of the division of normal-force load (fig. 11(a)) shows that the basic body carried about 21 percent of the total normal-force load whereas the indented body carried a slightly lesser amount (about 19 percent). Also shown in figure 11(a) is the normal-force coefficient for the body plus interference (the difference between the total normal-force coefficient and the wing normal-force coefficient). Results from the division of pitching-moment load (fig. 11(b)) show that the pitching-moment curves for the wing in the presence of the body exhibit a much more negative slope than the curves for the wing-body combination. A slight Mach number effect on the division of both normal-force and pitching-moment loads is also evident in figure 11.

A comparison of the experimental values from the basic body configuration and calculated values in accordance with references 6 and 7 of the lateral center-of-pressure position is presented in figure 12. Body interference was not included in these calculations. The calculated values at supersonic speeds show generally good agreement with the experimental values.

SUMMARY OF RESULTS

An investigation of the aerodynamic loading characteristics of a 60° delta wing in the presence of a basic and of an indented body has been conducted in the Langley 8-foot transonic pressure tunnel. The Mach number range was 0.6 to 1.2 and the angle-of-attack range was 0° to 20°. The data have been analyzed and indicate the following results for these delta-wing configurations.

1. With increases in C_{N_W} below pitch-up at a constant Mach number the center of pressure experiences no longitudinal movement and only small inboard movement above a Mach number of 0.94. At pitch-up, abrupt forward and inboard movements of the order of 4 percent of the mean aerodynamic chord and 3 percent of the wing semispan, respectively, are experienced.
2. With increases in Mach number at subsonic speeds at a constant C_{N_W} the center of pressure experiences small rearward and usually very slight outboard movements. In the transonic speed range this movement becomes larger and results in rearward and outboard center-of-pressure movements of the order of 7 percent of the mean aerodynamic chord and 3 percent of the semispan, respectively. No significant additional movement is evident at supersonic speeds.
3. Body indentation has no significant effects on the aerodynamic loading characteristics.
4. The effects of Mach number and body indentation on the division of loads are small.

Langley Aeronautical Laboratory,
National Advisory Committee for Aeronautics,
Langley Field, Va., June 28, 1955.

REFERENCES

1. Delano, James B., and Mugler, John P., Jr.: Transonic Wind-Tunnel Investigation of the Effects of Taper Ratio and Body Indentation on the Aerodynamic Loading Characteristics of a 45° Sweptback Wing in the Presence of a Body. NACA RM L54L28, 1954.
2. Platt, Robert J., Jr., and Brooks, Joseph D.: Transonic Wind-Tunnel Investigation of the Effects of Sweepback and Thickness Ratio on the Wing Loads of a Wing-Body Combination of Aspect Ratio 4 and Taper Ratio 0.6. NACA RM L54L31b, 1955.
3. Whitcomb, Richard T.: A Study of the Zero-Lift Drag-Rise Characteristics of Wing-Body Combinations Near the Speed of Sound. NACA RM L52H08, 1952.
4. Ritchie, Virgil S.: Effects of Certain Flow Nonuniformities on Lift, Drag, and Pitching Moment for a Transonic-Airplane Model Investigated at a Mach Number of 1.2 in a Nozzle of Circular Cross Section. NACA RM L9E20a, 1949.
5. Wiggins, James W.: Wind-Tunnel Investigation at High Subsonic Speeds of the Static Longitudinal and Static Lateral Stability Characteristics of a Wing-Fuselage Combination Having a Triangular Wing of Aspect Ratio 2.31 and an NACA 65A003 Airfoil. NACA RM L53G09a, 1953.
6. DeYoung, John, and Harper, Charles W.: Theoretical Symmetric Span Loading at Subsonic Speeds for Wings Having Arbitrary Plan Form. NACA Rep. 921, 1948.
7. Hannah, Margery E., and Margolis, Kenneth: Span Load Distribution Resulting from Constant Angle of Attack, Steady Rolling Velocity, Steady Pitching Velocity, and Constant Vertical Acceleration for Tapered Sweptback Wings with Streamwise - Subsonic Leading Edges and Supersonic Trailing Edges. NACA TN 2831, 1952.

TABLE I
BODY COORDINATES

Forebody		Afterbody			
Station, in. from nose	Radius, in.	Basic body		Indented body	
		Station, in. from nose	Radius, in.	Station, in. from nose	Radius, in.
0	0	22.500	1.875	22.500	1.875
.225	.104	26.500	1.875	23.000	1.874
.5625	.193	27.692	1.868	24.000	1.858
1.125	.325	28.692	1.862	25.000	1.832
2.250	.542	29.692	1.849	26.000	1.801
3.375	.726	30.692	1.825	27.000	1.766
4.500	.887	31.692	1.789	28.000	1.726
6.750	1.167	32.692	1.745	29.000	1.685
9.000	1.390	33.692	1.694	30.000	1.643
11.250	1.559	34.692	1.638	31.000	1.603
13.500	1.683	35.692	1.570	32.000	1.569
15.750	1.770	36.692	1.486	33.000	1.549
18.000	1.828	36.900	1.468	34.000	1.553
20.250	1.864	37.500	1.408	35.000	1.591
		38.500	1.298	35.500	1.585
		39.500	1.167	36.000	1.547
		40.500	1.030	36.900	1.468
		41.250	.937	Same as basic body coordinates from sta- tion 36.900 to sta- tion 41.250	

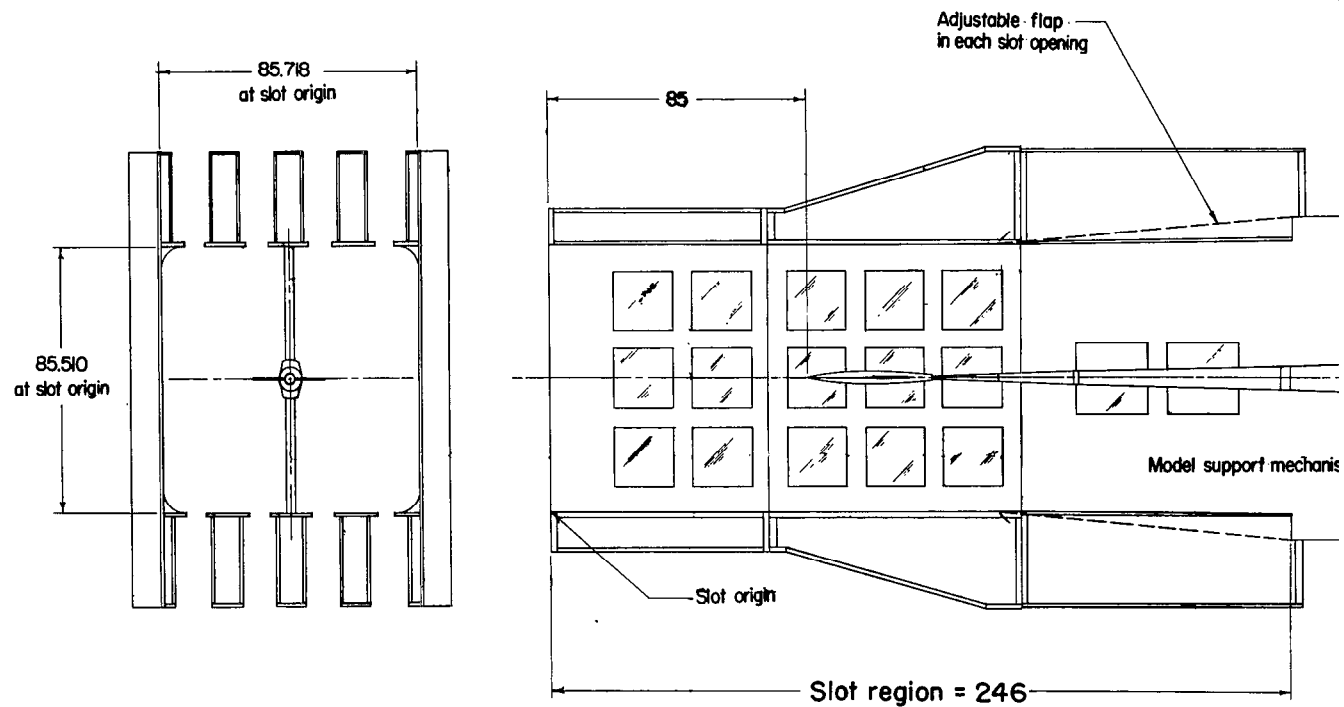


Figure 1.- Details of test section and location of model in the Langley 8-foot transonic pressure tunnel. All dimensions are in inches.

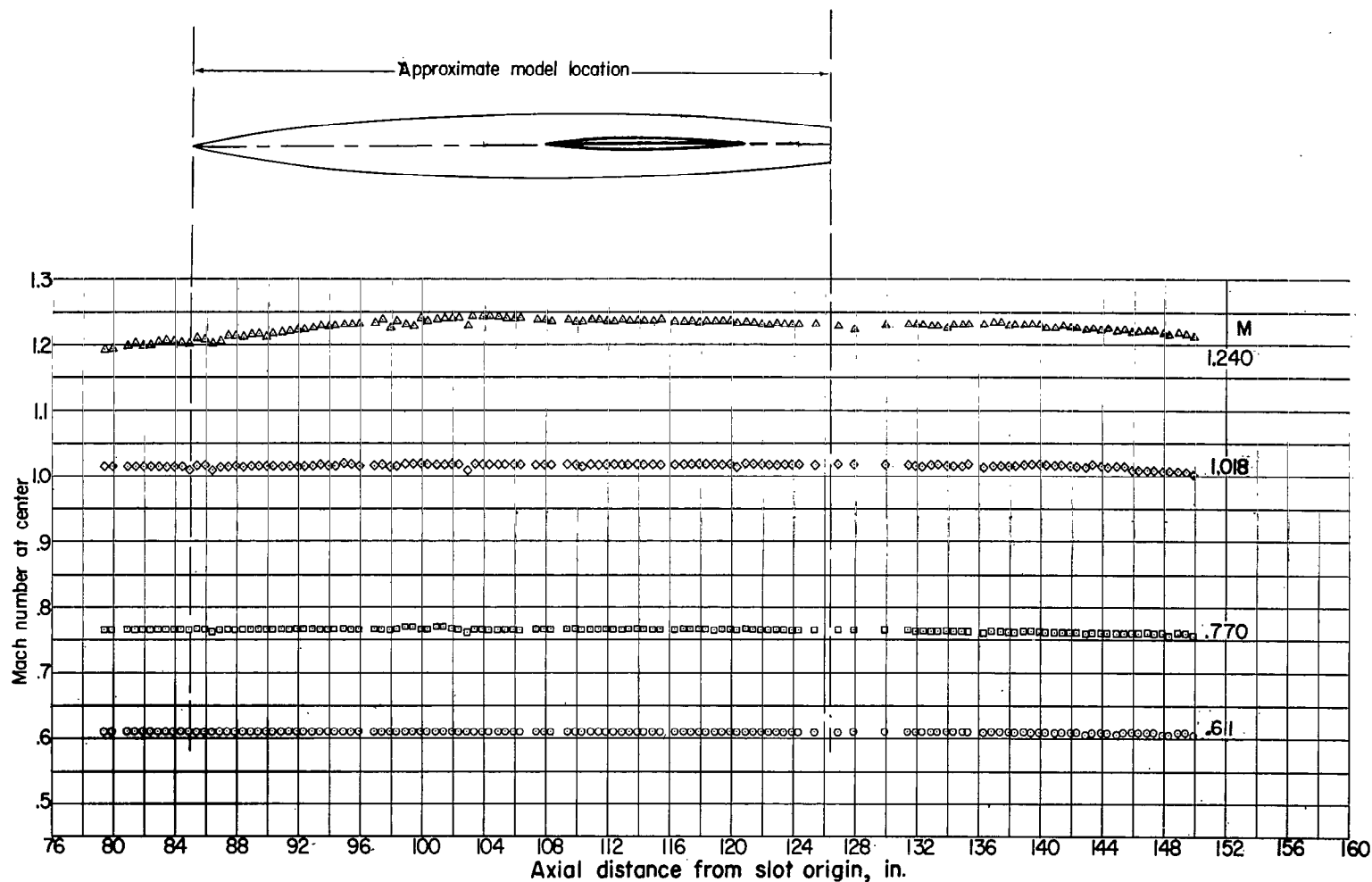
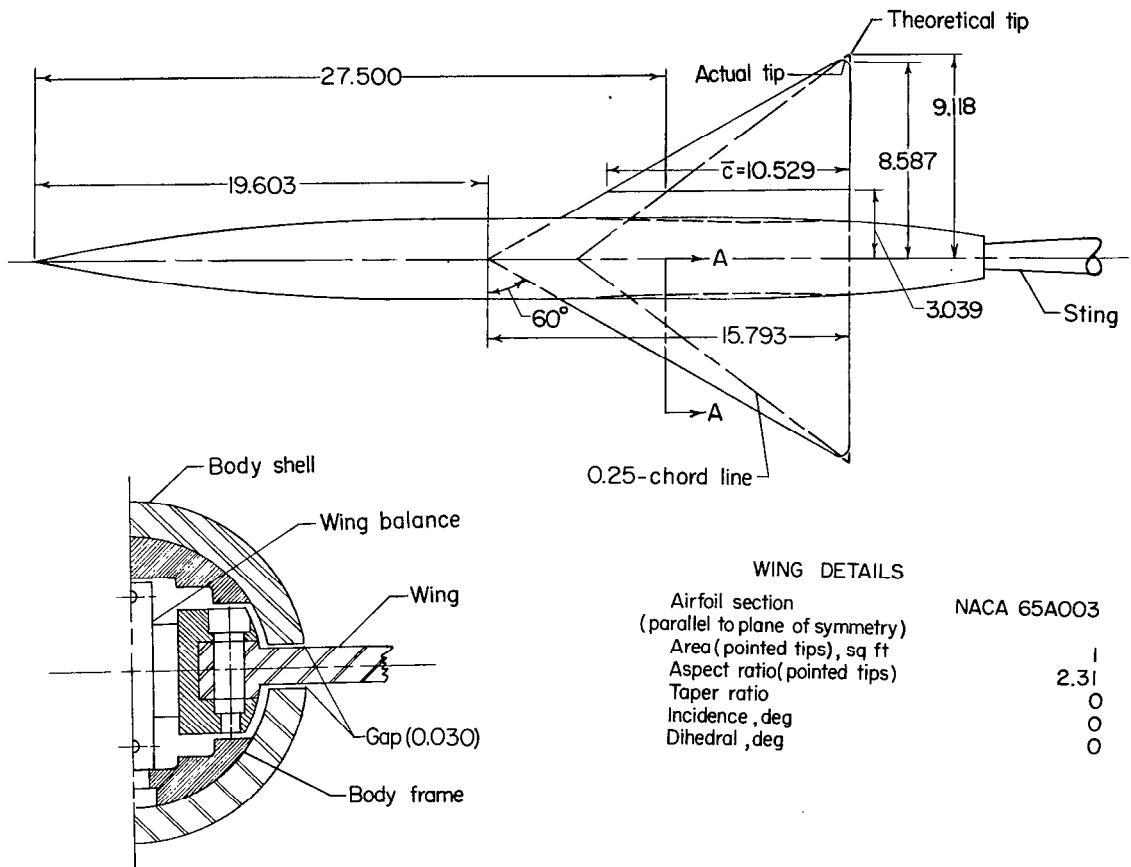


Figure 2.- Typical Mach number distributions in the test section of the Langley 8-foot transonic pressure tunnel.

9.118
8.587
.581



Section A-A enlarged to show detail of wing-body juncture

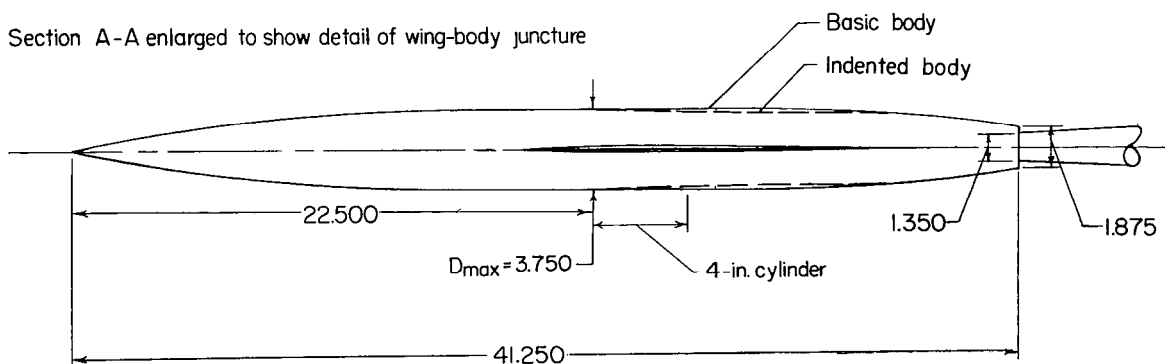


Figure 3.- Details of the wing-body configurations used in investigation.
All dimensions are in inches.

8.587
~~8.431~~
0.156
 9.118
 8.431
0.687

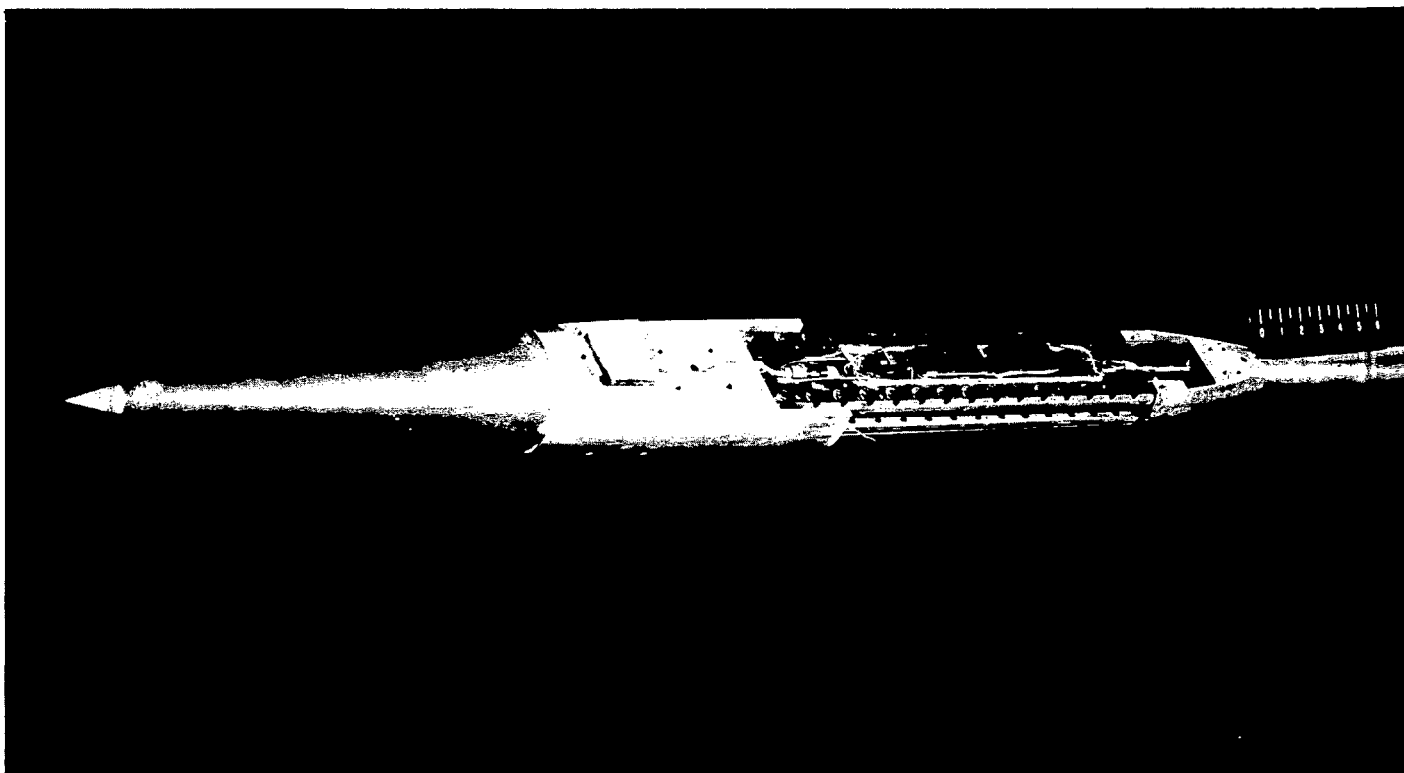


Figure 4.- Strain-gage balance mounted in the body. L-84807

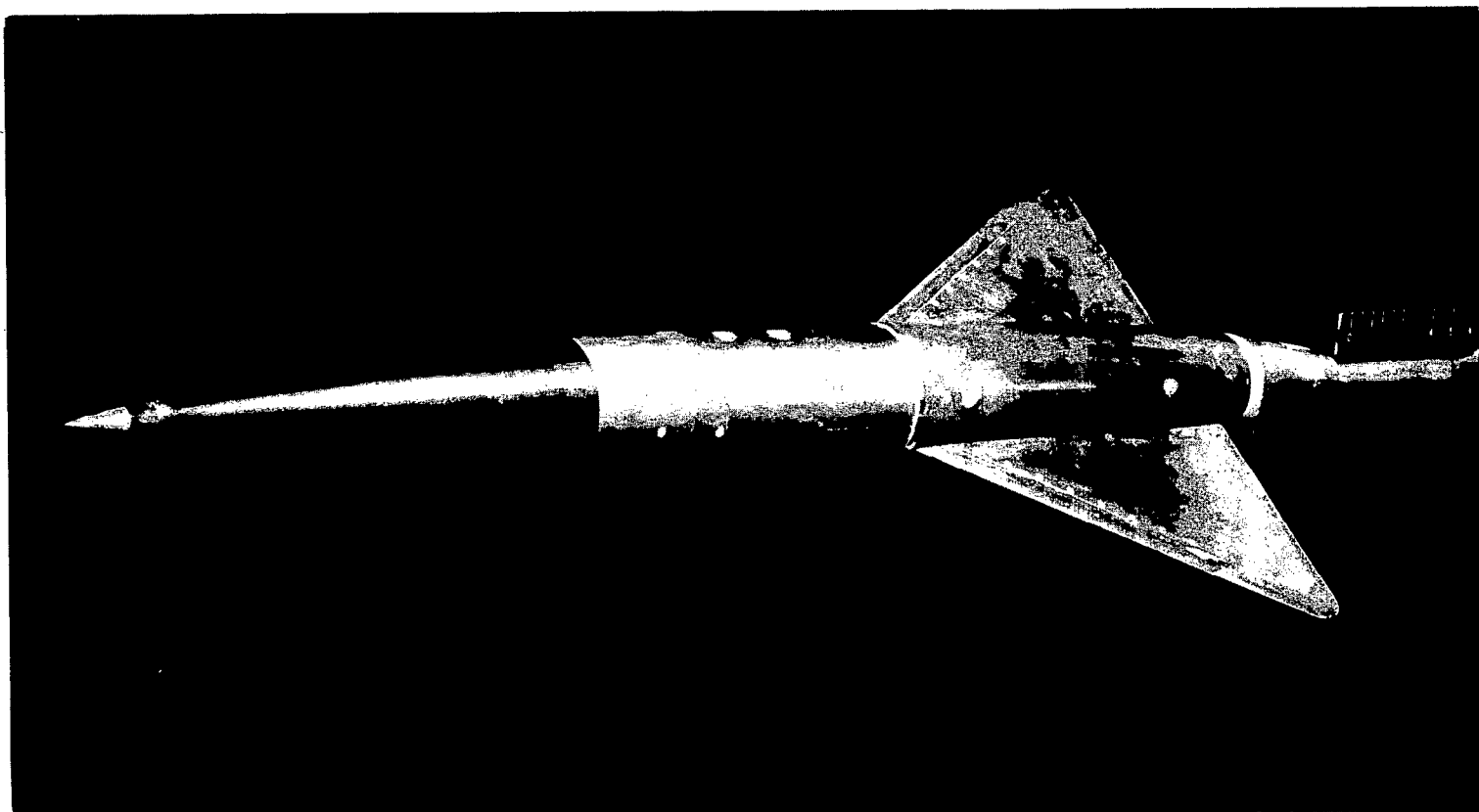


Figure 5.- Basic wing-body configuration.

L-84814

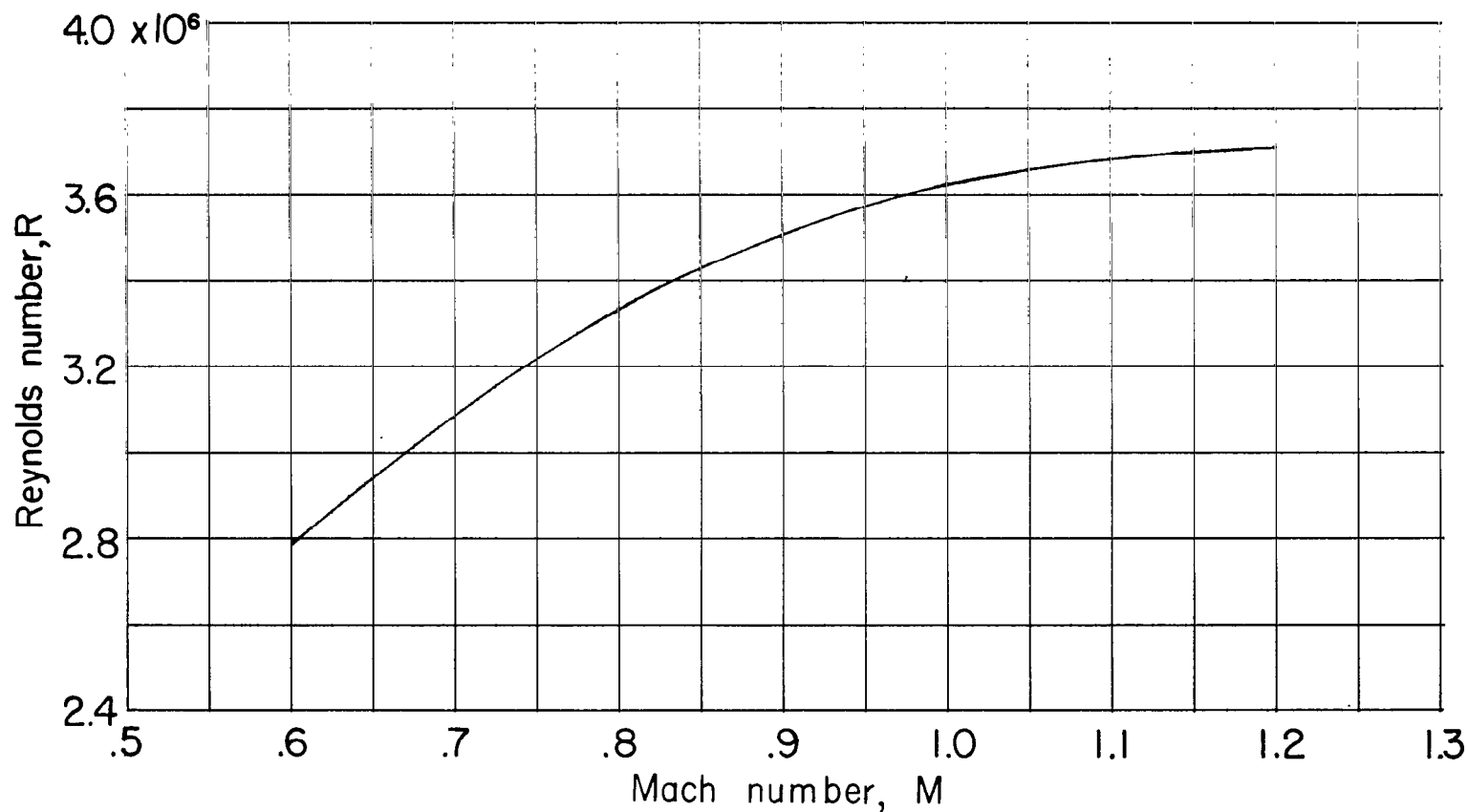
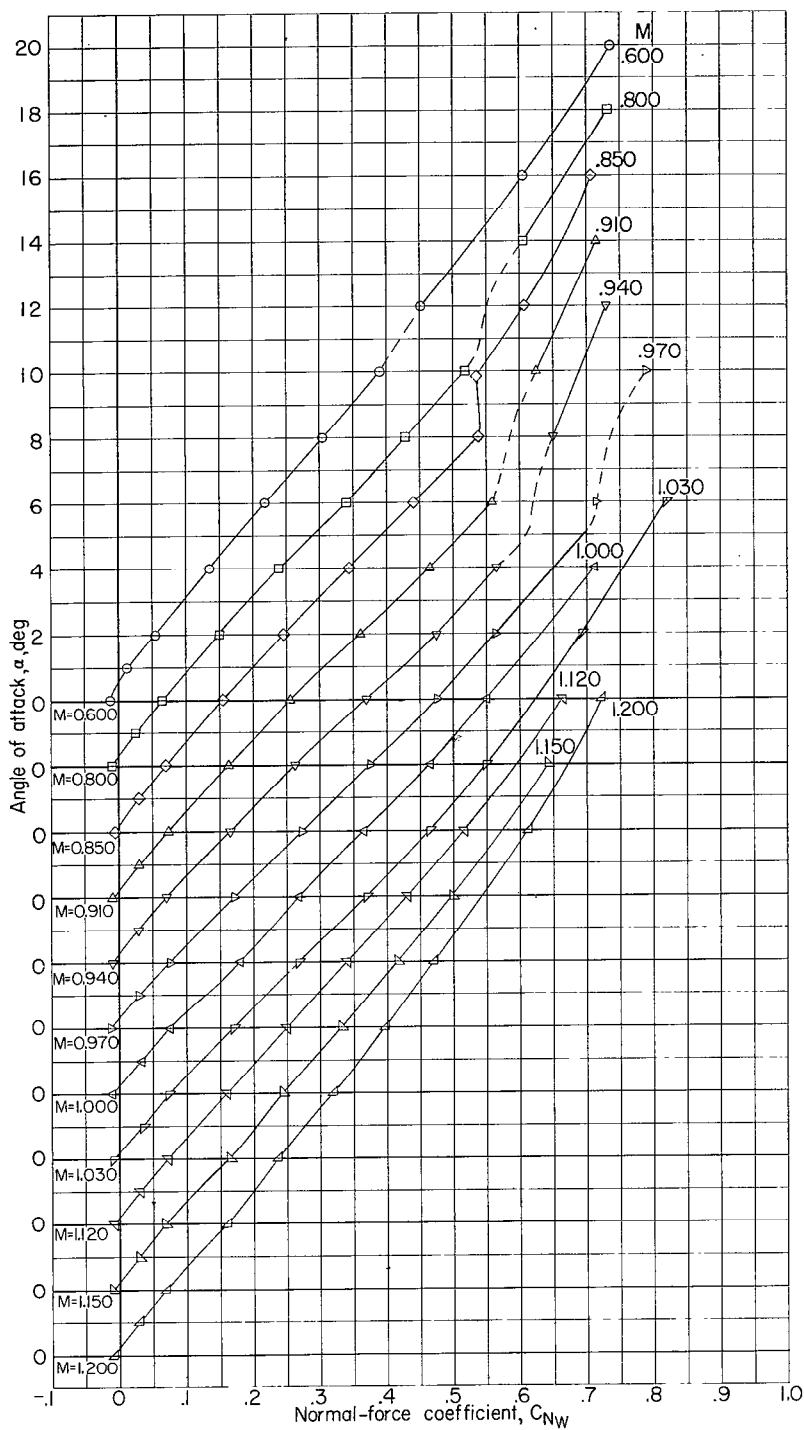
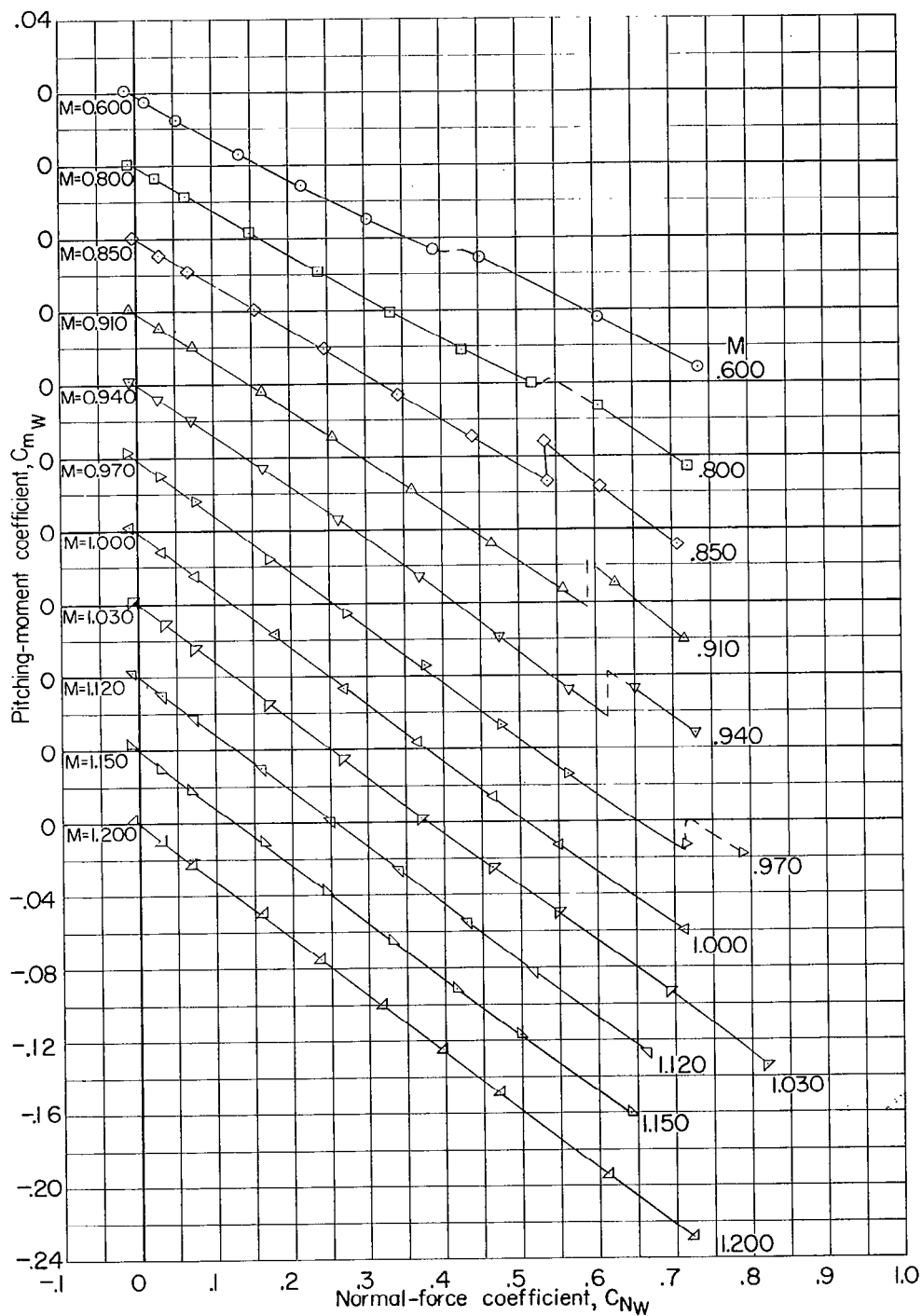


Figure 6.- Average variation with Mach number of Reynolds number based on the wing mean aerodynamic chord.



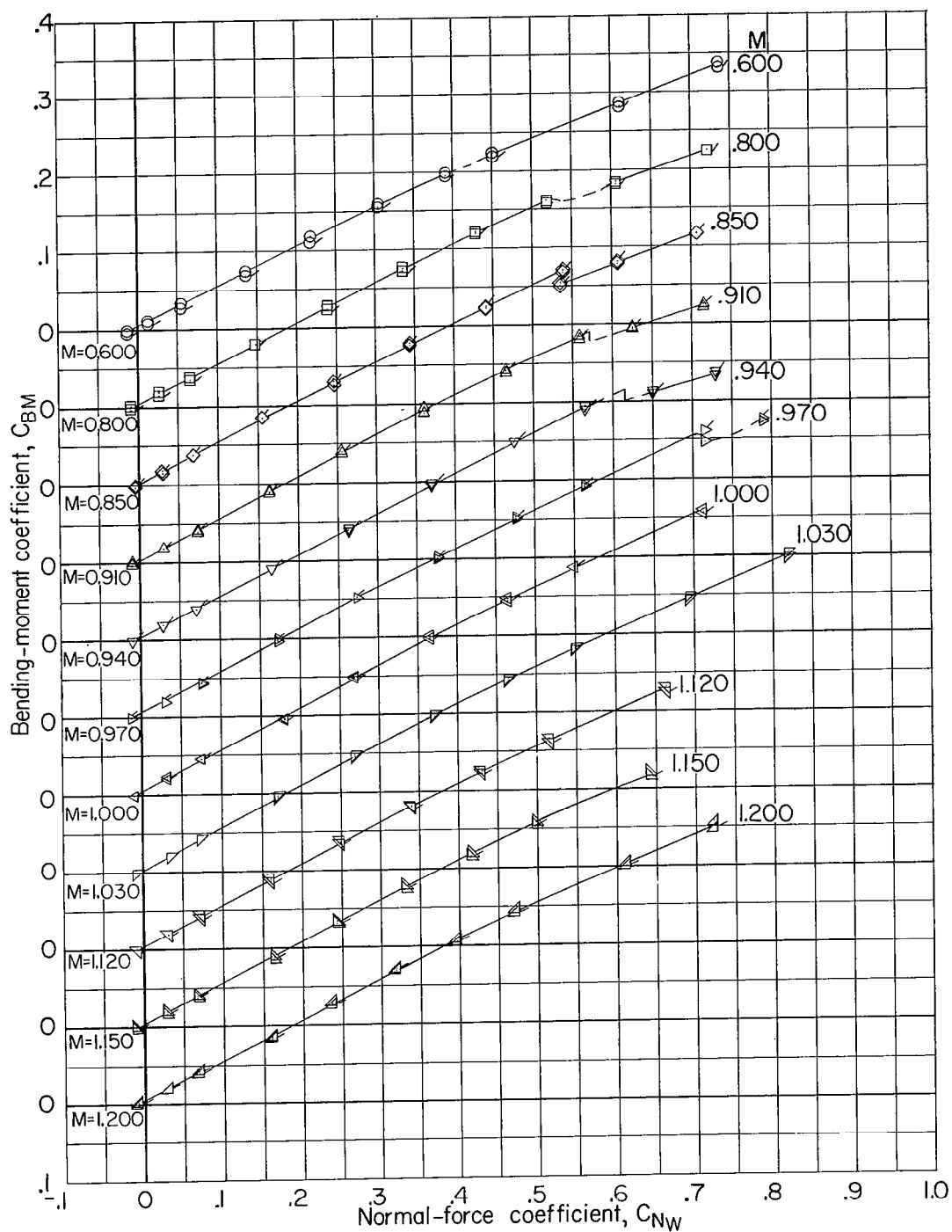
(a) Angle of attack.

Figure 7.- Aerodynamic characteristics of the wing in the presence of the basic body.



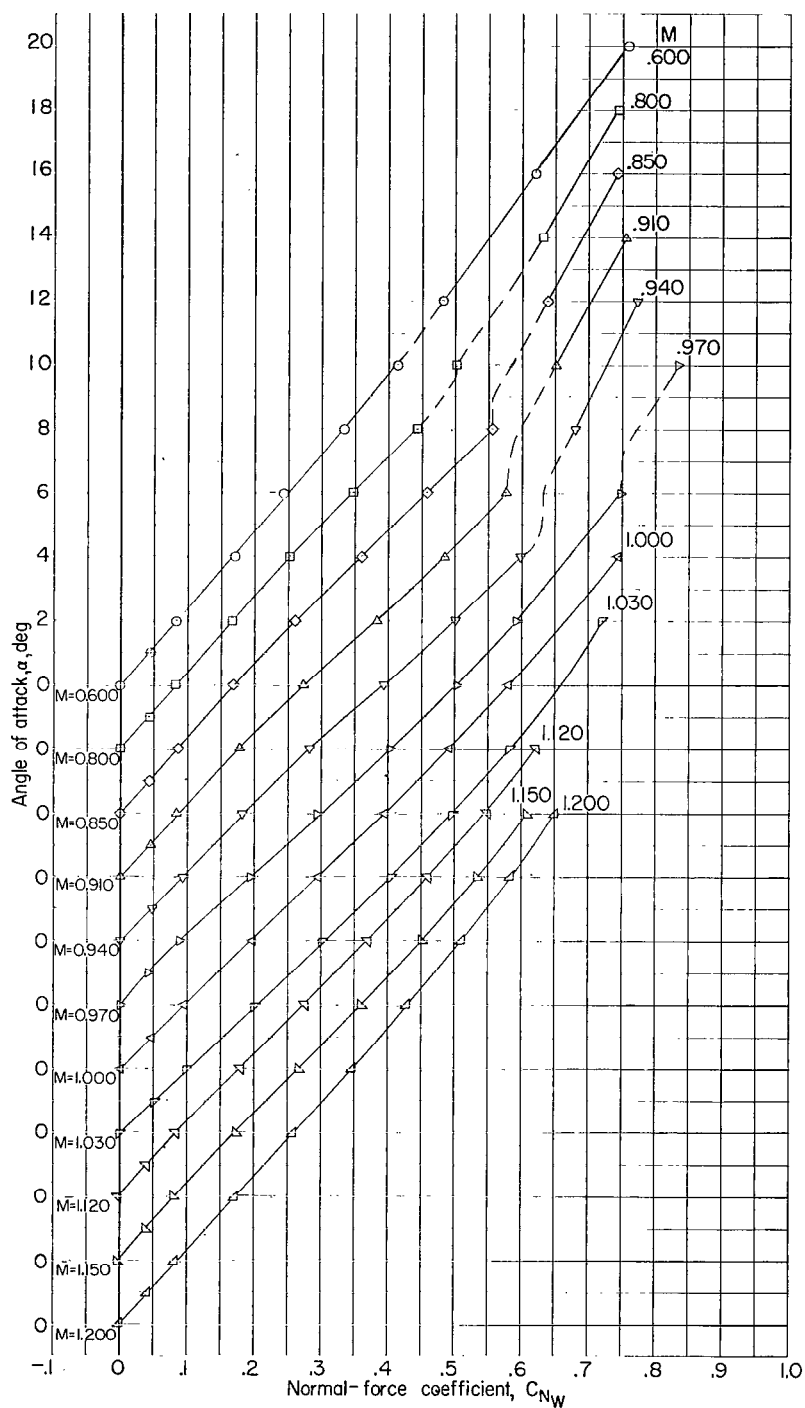
(b) Pitching-moment coefficient.

Figure 7.- Continued.



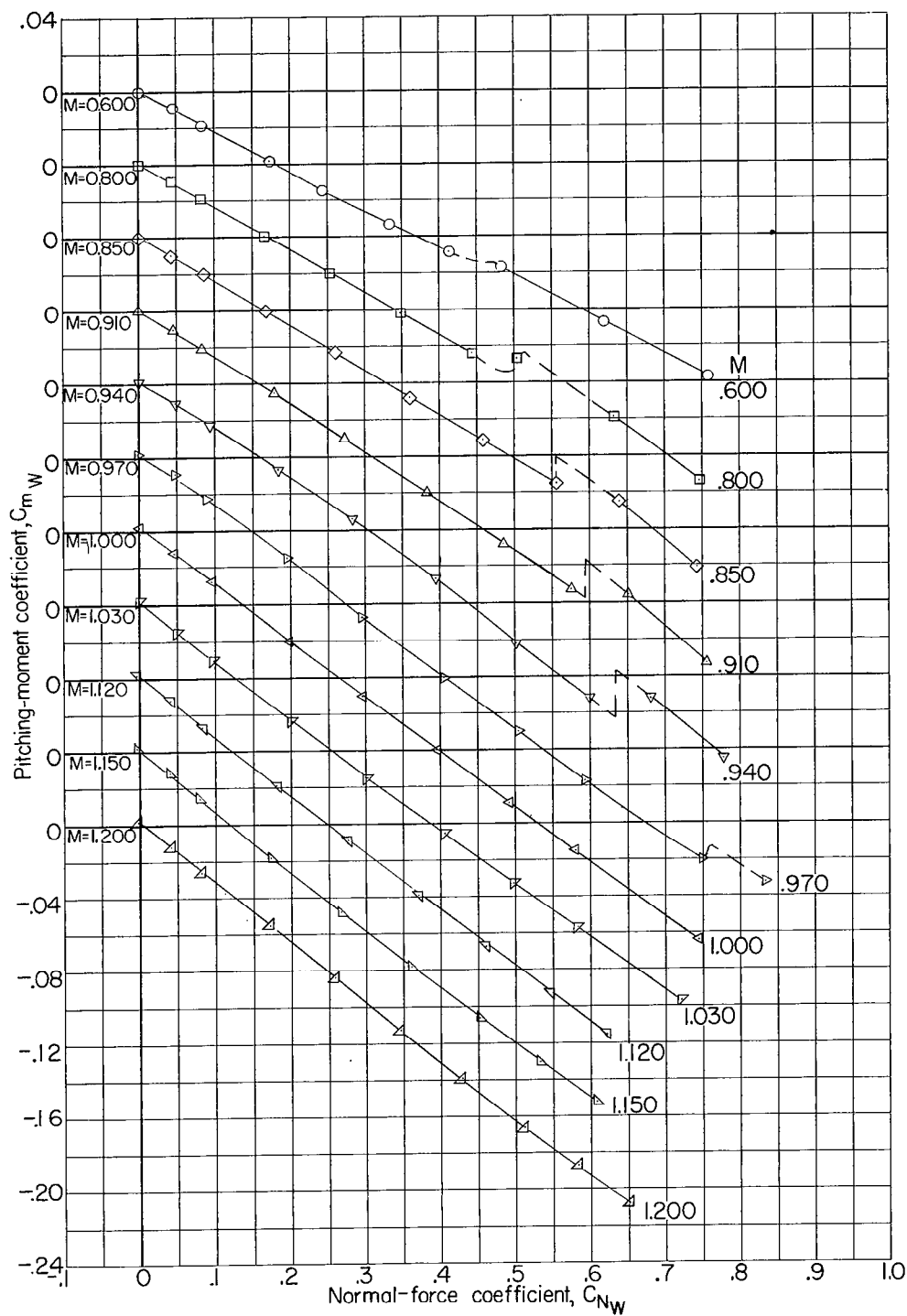
(c) Bending-moment coefficient. Plain and flagged symbols denote data for right and left wings, respectively.

Figure 7.- Concluded.



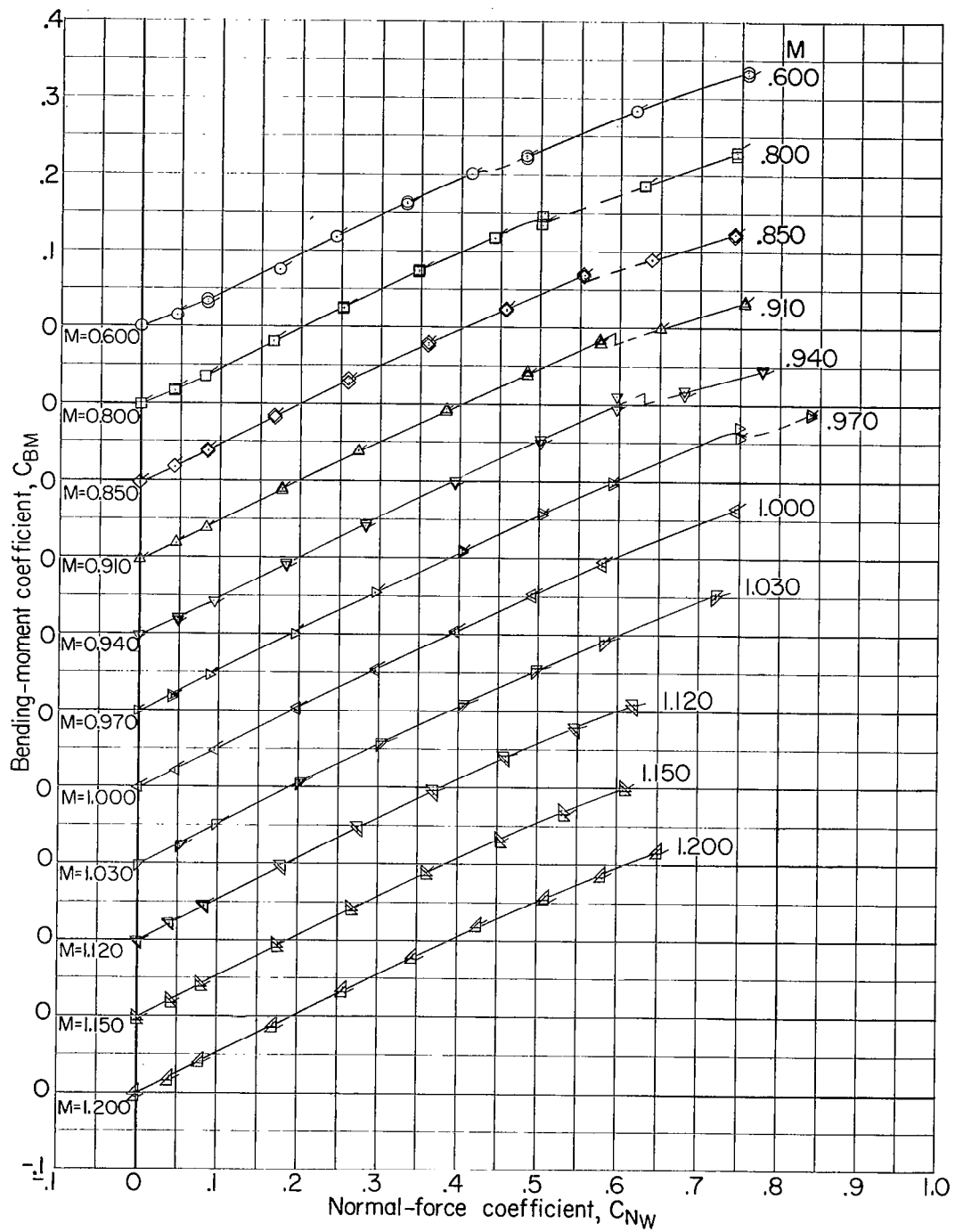
(a) Angle of attack.

Figure 8.- Aerodynamic characteristics of the wing in the presence of the indented body.



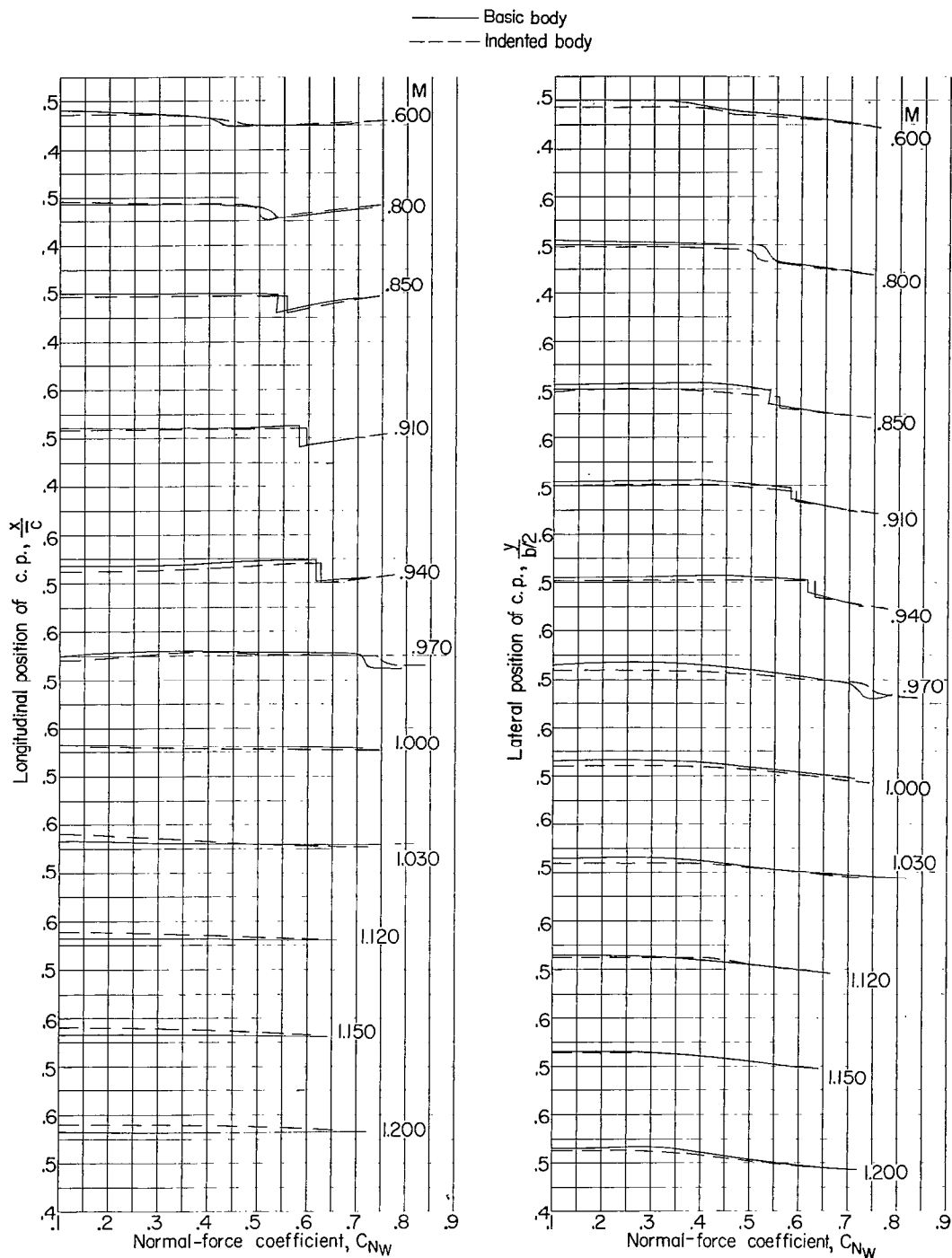
(b) Pitching-moment coefficient.

Figure 8.- Continued.



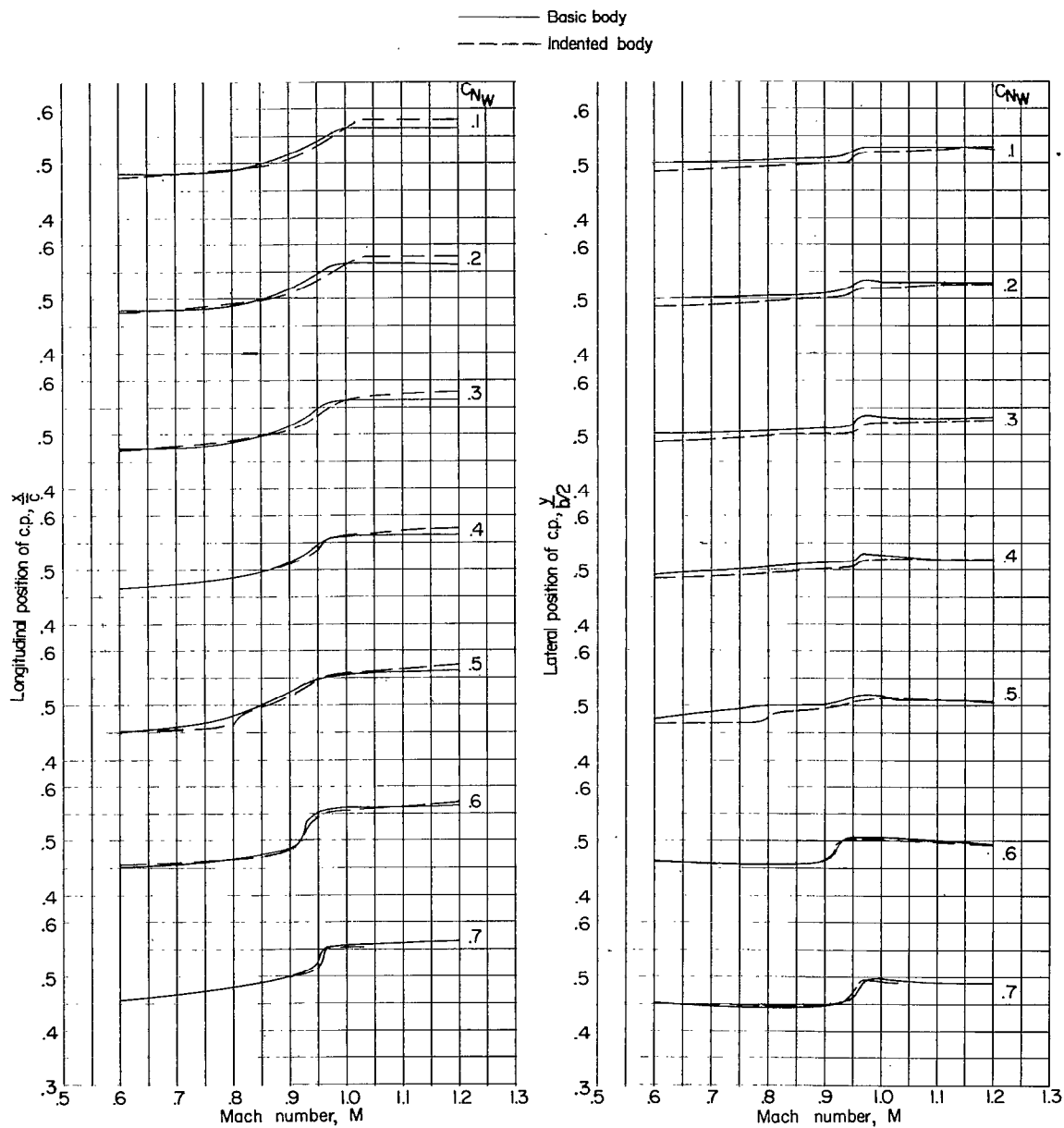
(c) Bending-moment coefficient. Plain and flagged symbols denote data for right and left wings, respectively.

Figure 8.- Concluded.



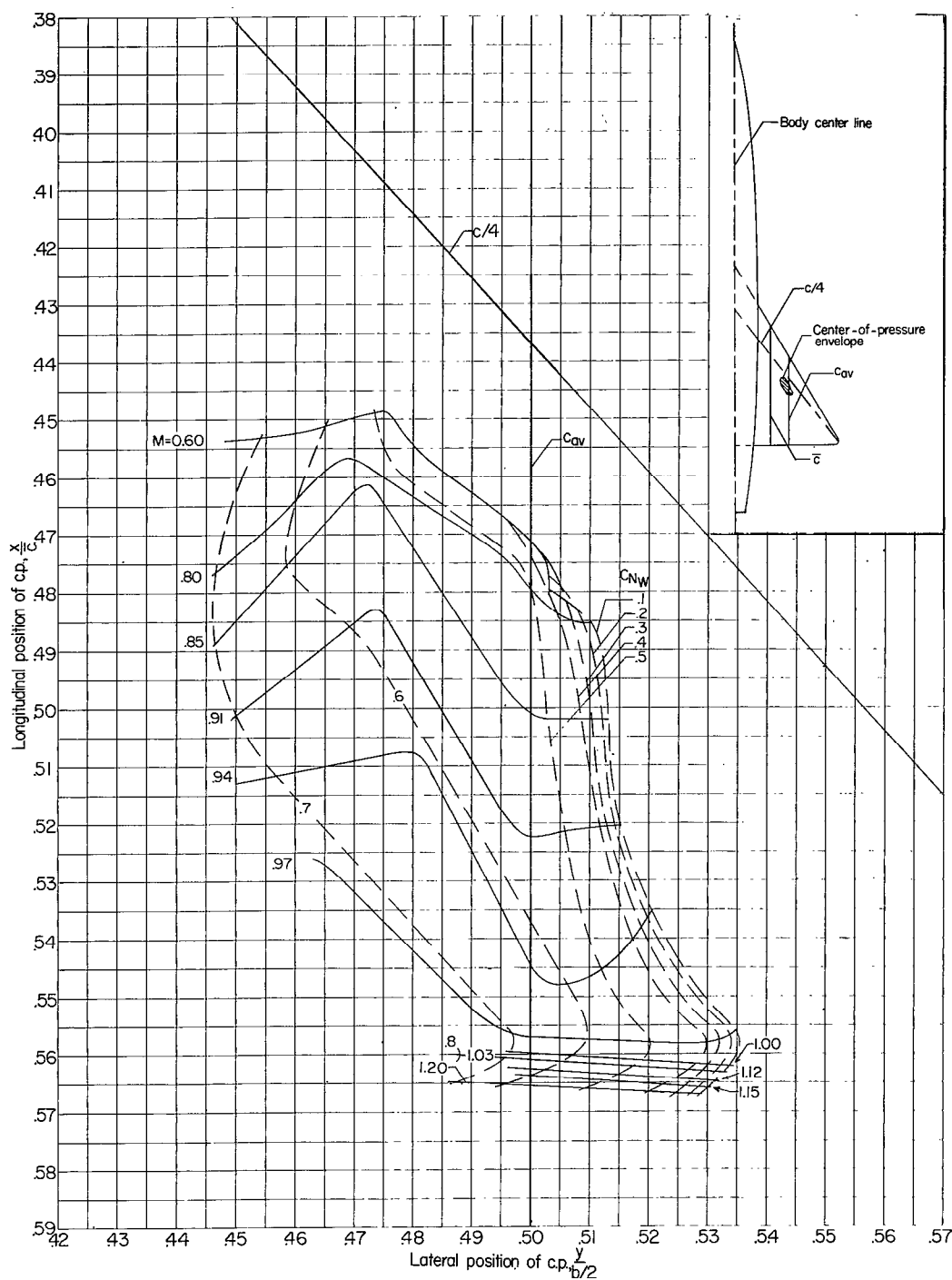
(a) Variation with wing normal-force coefficient.

Figure 9.- Effect of body indentation on the longitudinal and lateral position of the center of pressure for the wing in the presence of the basic and indented bodies.



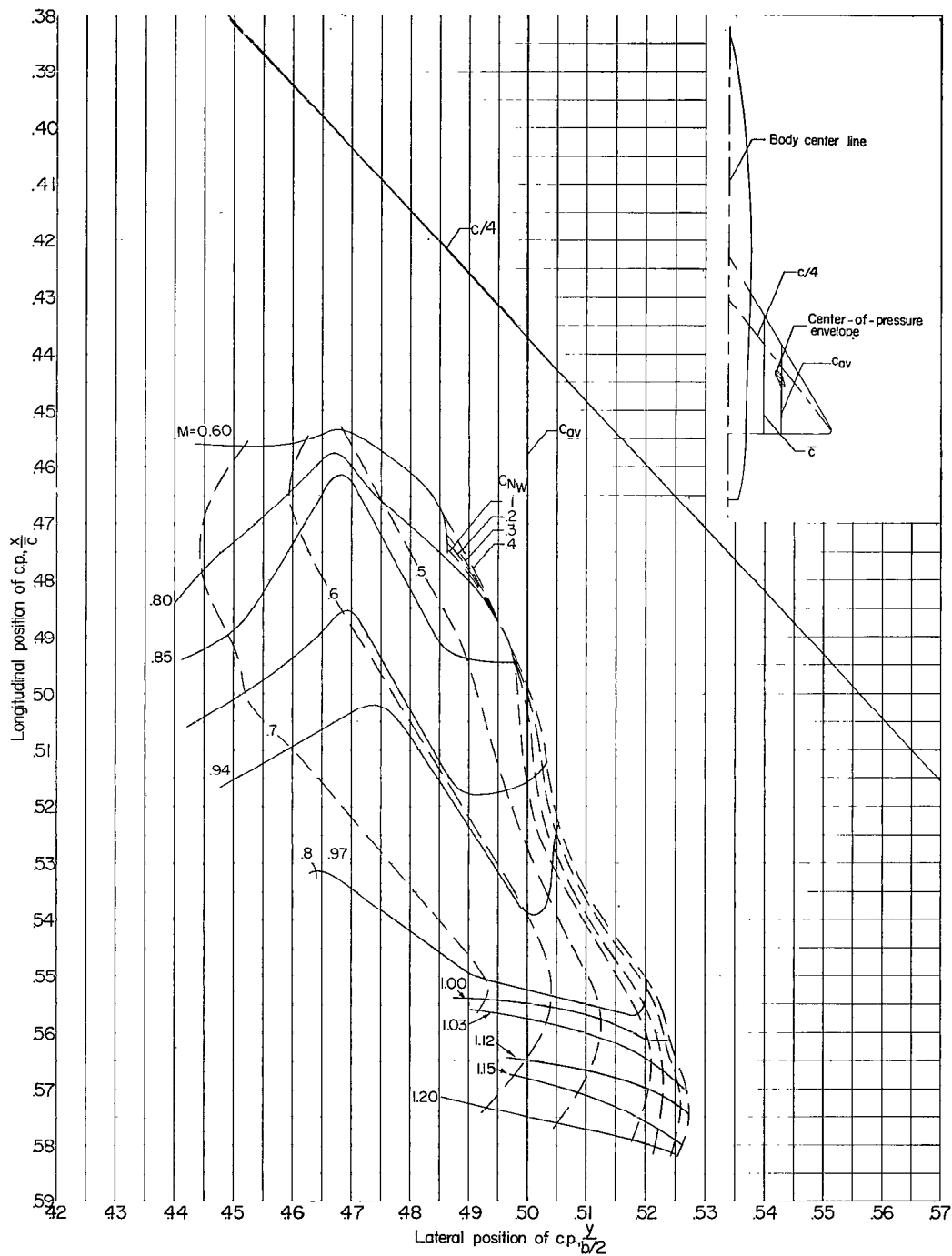
(b) Variation with Mach number.

Figure 9.- Concluded.



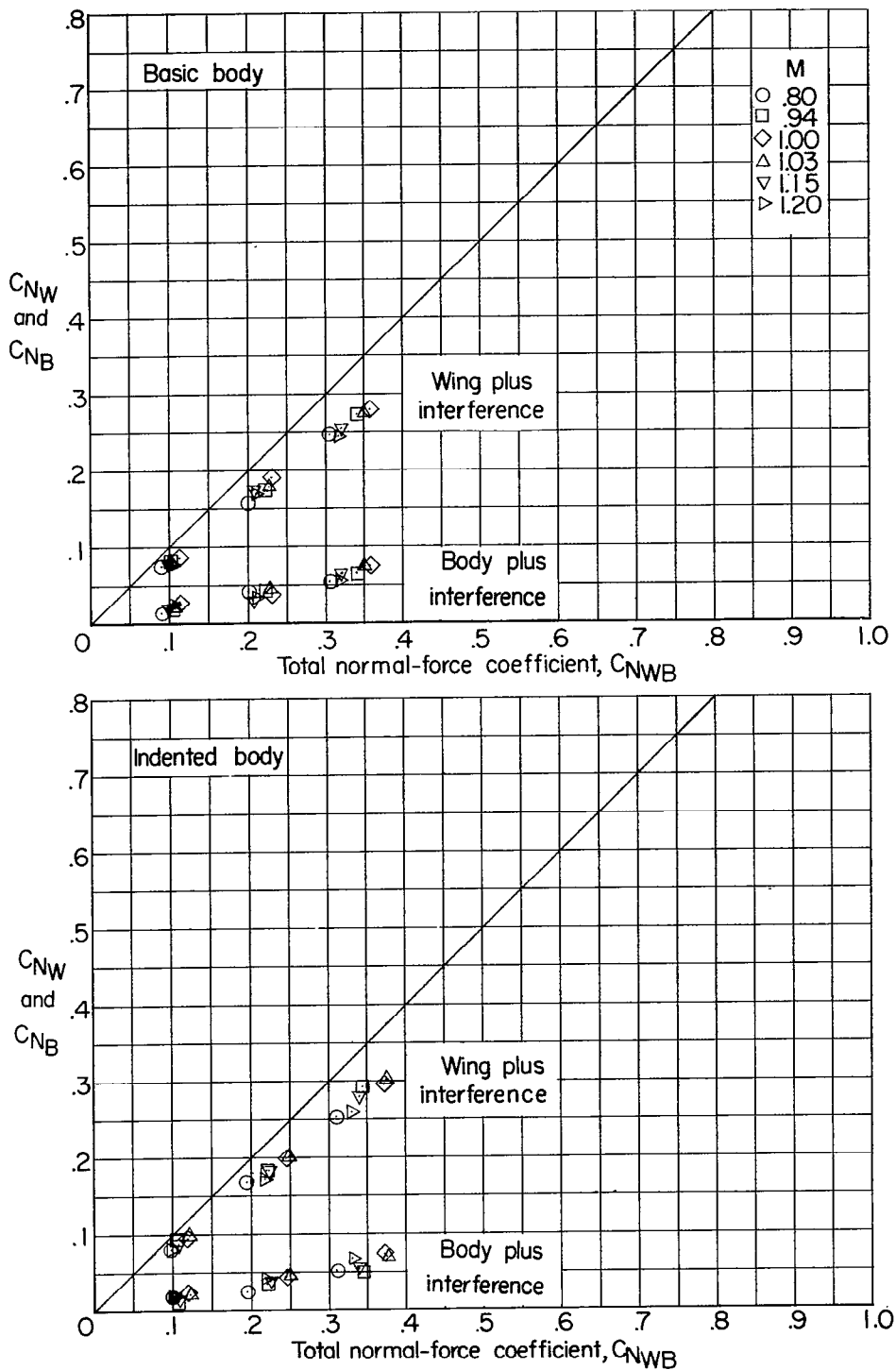
(a) Basic wing-body configuration.

Figure 10.- Variation with Mach number and wing normal-force coefficient of the longitudinal and lateral location of the center of pressure for the wing in the presence of the basic and indented bodies.



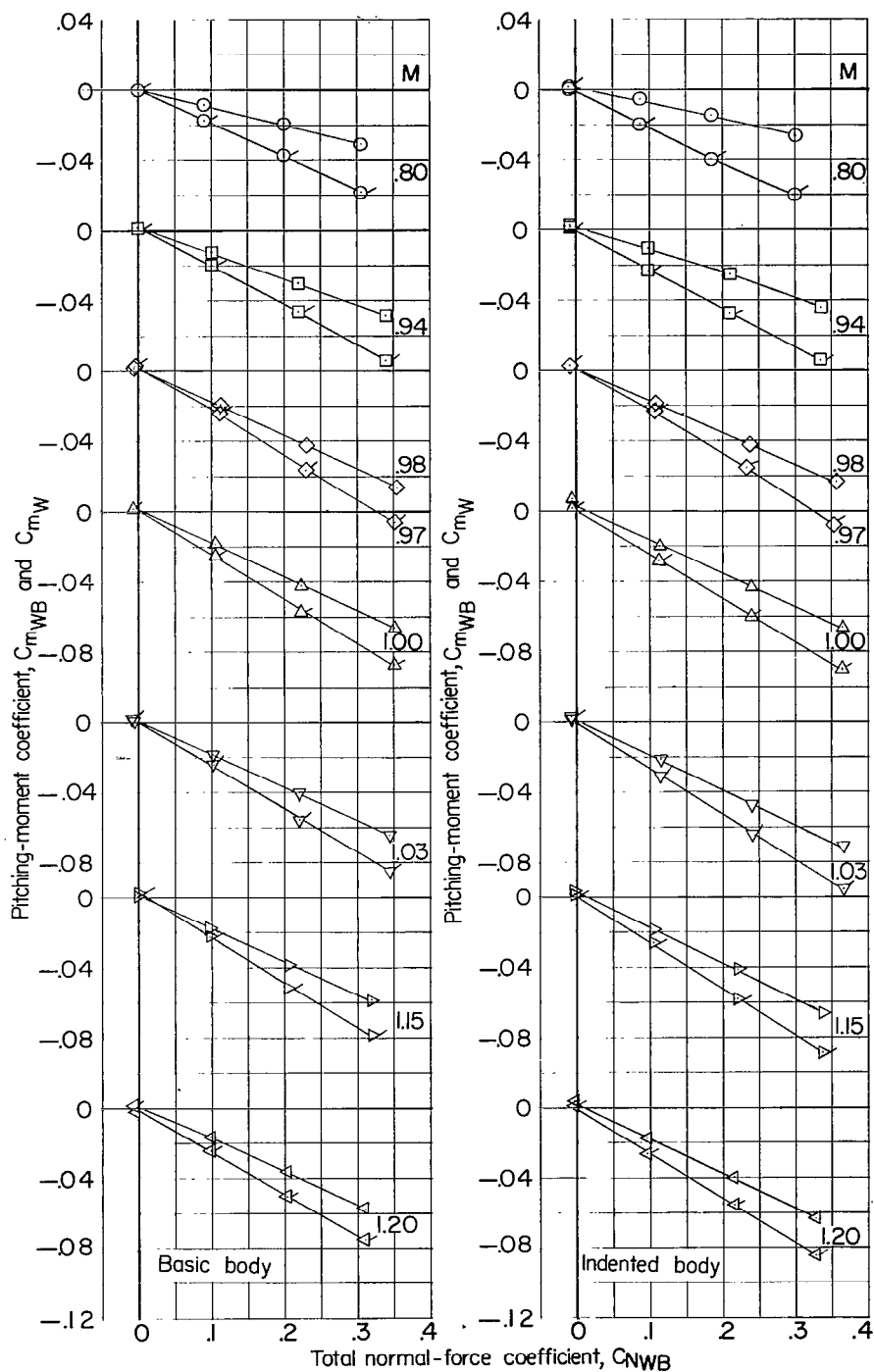
(b) Indented wing-body configuration.

Figure 10.- Concluded.



(a) Normal force.

Figure 11.- Division of load between the wing and body.



(b) Pitching moment. Plain symbols denote wing-body data; flagged symbols denote wing plus interference data.

Figure 11.- Concluded.

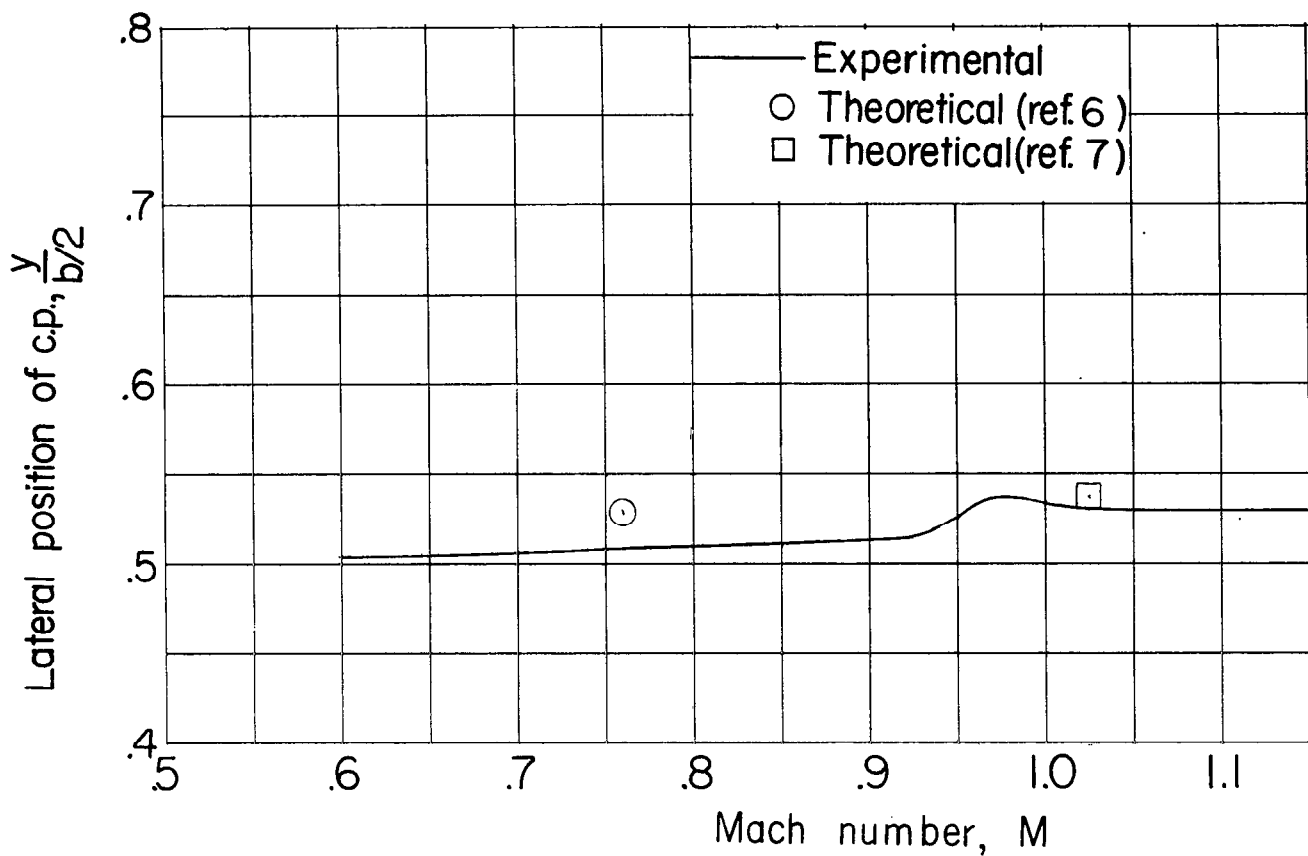


Figure 12.- Comparison of the experimental values from the basic bo configuration and calculated values of the lateral center-of-pre position. $C_{N_W} = 0.3$.